Synthesis and bactericidal properties of porphyrins immobilized in a polyacrylamide support: Influence of metal complexation on photoactivity.

Cinzia Spagnul,[a§] Lauren C. Turner,[a§] Francesca Giuntini,[b] John Greenman*[c] and Ross W. Boyle *[a]

[a] Department of Chemistry, University of Hull, Kingston-upon-Hull, East Yorkshire, HU6 7RX, UK

[b] School of Pharmacy & Biomolecular Sciences, Liverpool John Moores University, James Parsons Building, Byrom Street, Liverpool, L3 3AF, UK

[c] School of Life Sciences, University of the West of England, Bristol, BS16 1QY, UK

*corresponding author: E-mail: r.w.boyle@hull.ac.uk, Telephone: +44 (0)1482 466353, Fax: +44 (0)1482 466410

[§] Those authors have contributed equally and they are listed in alphabetic order.

Abstract

Spectroscopic and photodynamic properties of three novel polymeric hydrogels bearing porphyrins have been studied in vitro on the recombinant bioluminescent Gram-negative *Escherichia coli* DH5α to assess their ability to inactivate bacterial strains in solution.

The three different hydrogels were formed by polymerization of 5-[4-(2-(2-(2-acrylamidoethoxy)ethoxy)ethyl]carboxyphenyl-10,15,20-tris(4-*N*-methylpyridyl)porphyrin trichloride **(5)** and its complexes with Pd(II) **(6)** and Cu(II) **(7)** respectively, to form three optically transparent polyacrylamide hydrogels. All of the porphyrins are tricationic and they bear at the *meso* positions three *N*-methylpyridyl rings and one terminal acryloyl group connected through a flexible hydrophilic linker, particularly suitable for the later polymerization and incorporation into a hydrogel.

The hydrogels were characterized by IR and scanning electron microscopy and incorporation of the dye was confirmed by UV-visible spectroscopy.

All the hydrogel are characterized by a non-ordered microporous structure. The *E. coli* exhibited a decrease of 1.87 log after 25 mins irradiation when the porphyrin hydrogel **9** was evaluated. When the Pd(II) and Cu(II) porphyrin hydrogels were tested **(10, 11)**, they showed a 2.93 log decrease and 1.26 log decrease in the survival of the *E. coli* after 25 mins irradiation, respectively.

Similar results were obtained when the porphyrins were tested in solution. Of the three hydrogels, the Pd(II) porphyrin hydrogel **(10)** proved to be the one with the highest photokilling ability under illumination, and also exhibited the lowest toxicity in the absence of light. Hydrogels **9** and **10** were found to be active for five cycles, suggesting the possibility of reuse.

Introduction

Antimicrobial resistance is a complex global public health challenge,[1] making treatment of an increasing range of infections caused by bacteria, parasites, viruses and fungi difficult. The reduced efficacy of the existing drugs makes the treatment of patients inefficient, costly, or even impossible. The impact on particularly vulnerable patients is most obvious, resulting in prolonged illness and increased mortality. Furthermore a longer duration of illness and treatment, often in hospitals, increases healthcare costs as well as the economic burden on families and societies.

The current lack of new antimicrobials on the horizon to replace those that become ineffective brings added urgency to find alternative techniques that reduce microbial infections.

Photodynamic Antimicrobial Chemotherapy (PACT) is a very promising alternative. It relies on the combination of molecular oxygen ($^3O_2$) with a photosensitiser (PS, ideally non-toxic).[2,3,4] The photodynamic process involves the activation of the photosensitiser to its excited triplet state by non-thermal visible light of appropriate wavelength(s) (visible light or sunlight). The excited photosensitiser either promotes ground state molecular oxygen ($^3O_2$) to highly reactive singlet oxygen ($^1O_2$) by energy transfer, or generates oxygen radicals by electron transfer, thus producing reactive oxygen species (ROS) which are responsible for the bacterial killing. PACT has additional advantages over alternative techniques, as it is known to kill multi-antibiotic resistant strains as well as native strains,[5] avoiding the problem of microbial resistance.[6,7] and because no induction of resistance after multiple treatments has been reported.[8]

During the last 20 years several types of photosensitisers have been tested for PACT purposes, such as porphyrins, phenothiazinium dyes, Rose Bengal, ruthenium complexes, phthalocyanines and BODIPY[9] both in solution[10] or immobilized onto a surface.[11]

Porphyrins are known to effectively produce ROS upon visible light irradiation,[12] and therefore have been intensively studied as photo-bactericidal agents against both Gram-negative and Gram-positive bacteria,[13] although Gram-negative bacteria are less prone to be killed due to the complex

architecture of their bacterial cell membrane, that intercept $^1O_2$ and acts as an effective barrier to the penetration into the cell of many photosensitising dyes.[14] Only cationic dyes allow an extensive photo-induced inactivation of both types of bacteria.

When immobilized in solid supports, cationic porphyrins were found to be effective against both Gram-positive and Gram-negative bacteria, such as *E. coli, M. smegmatis, P. aeruginosa, B. subtilis*, *E. faecalis, V. fischeri,* and on *S. aureus, A. baumannii,* and their multiresistant strains *S. aureus (MRSA), A. baumannii (MDRAB).*[11,13] They were found to be effective also against viruses such as *Influenza A virus* and fungi such as *C. albicans*.[11,13,15]

The attachment of porphyrins to natural and synthetic polymers has been extensively investigated. The immobilization of the PS on a solid support offers the advantage of recovering and possibly reusing of the PS, making the materials very interesting for an eco-friendly approach.

Porphyrins have been incorporated into natural polymers, such as cellulose, cellulose paper, cotton fabric, nanocrystalline cellulose as well as in synthetic polymers, such as polythiophene polydimethylsiloxane, indium tin oxide films, silica magnetic nanoparticles, polyamide 6, polyurethane, polystyrene, polycaprolactone and the photoantimicrobial ability of the resulting materials evaluated.[11]

The field still faces the key challenge of having a photobactericidal material with significant activity and with the dye present at the lowest concentration possible, minimizing the leaching and with an improved durability of the material.

Recently, we have successfully prepared an optically transparent polyacrylamide hydrogel loaded with a new phenothiazinum compound with antibacterial properties that were activated by light.[16]

The photoactive gel successfully killed both Gram-positive and Gram-negative bacteria, such as *S. aureus* and *E. coli* and the use of bioluminescent target species allowed many variables to be tested such as the effects of increasing the amount of hydrogel used in the same experiment, increasing the interactive surface area between target cells and immobilized gel, and the recovery and further testing of gel through five cycles of fresh challenges.

In the present study, we used the same polyacrylamidic support to covalently immobilize three new cationic porphyrins (Figure 1). The killing ability of those new antibacterial hydrogels was then evaluated and compared.

As previously reported,[17] we used a rapid method to assess the antibacterial effect of the hydrogel system by the real-time reduction in the light output of recombinant bioluminescent *E. coli* DH5α under artificial irradiation.

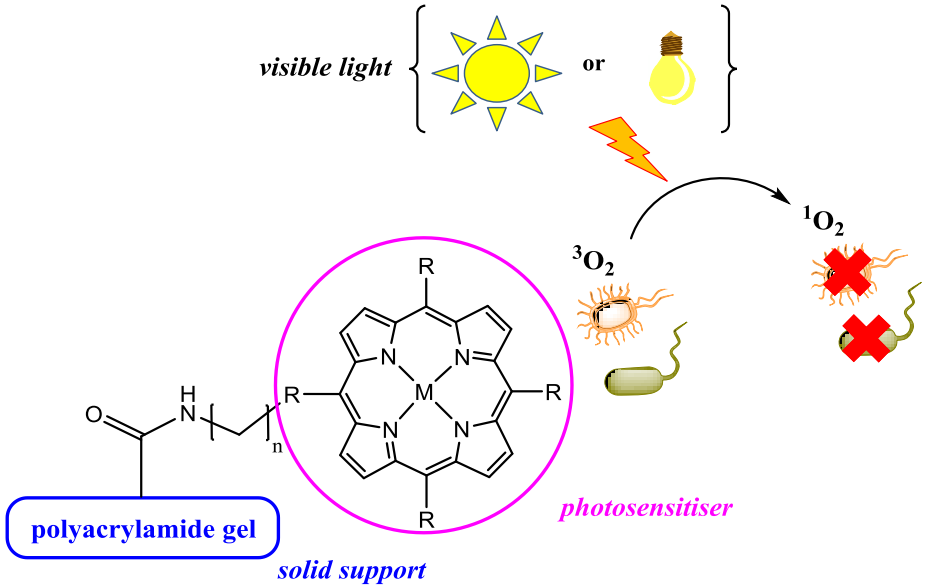

Figure 1: Schematic drawing of the photodynamic inactivation of microorganisms by singlet oxygen generated by the photosensitiser immobilized on a polyacrylamide support.

Experimental

Mono and bidimensional (H–H COSY), ^{1}H NMR spectra were recorded at ambient temperature on a JEOL Eclipse 400 and JEOL Lambda 400 spectrometers (operating at 400 MHz for ^{1}H and 100 MHz for ^{13}C). In all the solvents chemical shifts were referenced to the peak of residual non-deuterated solvent (d = 7.26 for $CDCl_3$, 4.89 for D_2O, 2.50 for DMSO-d_6). Coupling constants (J values) are reported in Hertz (Hz) and are H–H coupling constants unless otherwise stated. Assignments were performed through conventional 2D correlation spectra.

UV-visible spectra were obtained at T = 25 °C on a Varian Cary 50 Bio UV-vis spectrophotometer using 1.00 cm path-length quartz cuvettes (3.00 mL).

UV-visible spectra of the solid samples were obtained on the same spectrophotometer used for samples in solution. The solid UV-visible spectra were obtained by forming the gels inside the cuvette.

Infrared spectra were obtained on a Nicolet IS5 Spectrometer with an iD7 diamond ATR attachment operating in ATR mode with frequencies given in reciprocal centimeters (cm^{-1}).

Mass spectra of all compounds were obtained from the EPSRC National Mass Spectrometry Service, Swansea.

All reactions were monitored by thin-layer chromatography (TLC) on pre-coated SIL G/UV254 silica gel plates (254 mm). Column chromatography was performed on silica gel 60 A (40–63 micron), eluting with dichloromethane/methanol mixtures as specified below. Commercial solvents and reagents were used without further purification unless stated otherwise. Chemical reagents were purchased from Sigma-Aldrich, Fluka, Acros, Fluorochem and Alfa Aesar at the highest grade of purity available, and were used as received, unless otherwise stated. All other solvents were purchased from Fisher Scientific and used as received. Solvents were dried according to a procedure by Williams *et al*., where the solvent was dried over molecular sieves and changed as necessary.[18]

N-{2-[2-(2-aminoethoxy)ethoxy]ethyl}acrylamide **(3)** was prepared as described by us in reference 16.[16]

The porphyrins precipitate with variable amounts of anti-solvent that depends on the batch. For this reason, elemental analysis of such conjugates did not afford reliable and reproducible results and the values are not reported here (typically, some of the elemental analysis values, especially for C, differ from calculated values by >0.5%). Nevertheless, the purity calculated from elemental analysis data was always >95%, and the proposed formulas are all consistent with the ^{1}H NMR and the mass spectra.

High performance liquid chromatography (HPLC) analysis was carried out on a Jasco system equipped with a Jasco PU-1580 dual pump, Jasco MD-1515 multi-wavelength detector and a Gemini- NX C18 column (100 A, 150 x 4.6 mm) using as the mobile phase 0.1% trifluoroacetic acid in water (solvent A) and 0.1% trifluoroacetic acid in acetonitrile (solvent B).The gradient elution was 5% A and 95% B in 18 mins with a flow rate of 1.00 mL min^{-1} and the injection volume was 10.00 µl. All microwave reactions were conducted using a CEM discover SP microwave reactor at 150 W unless stated otherwise. All programmes used maximum stirring and maximum pressure of 200 bar with 1 minute pre-stirring. Reaction temperatures were monitored using an external IR temperature probe and carried out in 35 mL sealed reaction vessels.

Synthesis and characterization of compounds

5-(4-carboxymethylphenyl)-10,15,20-tris(4-*N*-pyridyl)porphyrin (1): A procedure from the literature[19] was modified as follows: to a stirred refluxing solution of methyl-4-formylbenzoate (3.69 g, 22.5 mmol, 1.0 equiv.) and 4-pyridinecarboxaldehyde (6.40 mL. 67.9 mmol, 3.0 equiv.) in propionic acid (500 mL) was added drop-wise, *via* syringe, pyrrole (5.54 mL, 79.9 mmol, 3.7 equiv.). The reaction mixture was heated at reflux for an hour, then cooled to room temperature and the excess solvent was removed under reduced pressure. Thin layer chromatography of the crude product (dichloromethane/methanol 95.5:4.5) showed it to be a mixture of the six possible

porphyrin isomers that were separated by column chromatography on silica gel (dichloromethane/methanol 95.5:4.5).

The title porphyrin was identified by TLC comparing its Rf value (0.34) with that of a pure sample. The product was precipitated from methanol over dichloromethane to give a purple solid (720 mg, 4.7 % yield).

$\lambda_{max}(CH_2Cl_2, 25°C)$/nm 415 (ε/$dm^3$ mol^{-1} cm^{-1}664580), 515 (43985), 590 (13342) and 645 (5423).

^1H (400 MHz, $CDCl_3$) δ: − 3.00 (2H, s, N*H*), 4.13 (3H, s, OCH_3), 8.15-8.18 (6H, m, 3,5Py), 8.30 (2H, d, *J* = 8.0 Hz, *o*Ph,), 8.47 (2H, d, *J* = 8.0 Hz, *m*Ph), 8.84-8.89 (8H, m, βH), 9.04-9.08 (6H, m, 2,6Py).

^{13}C (100 MHz, $CDCl_3$) δ: 167.25, 149.95, 148.54, 146.34, 134.61, 134.61, 130.08, 129.43, 128.18, 120.19, 117.75, 117.55, 52.64.

ESI-MS (*m/z*) ($CHCl_2$/MeOH + NH_4OAc): calcd. for $C_{43}H_{30}N_7O_2$: 675.24 found $[M+H]^+$: 676.2455.

5-(4-carboxyphenyl)-10,15,20-tris(4-*N*-pyridyl)porphyrin (2): A procedure from the literature was modified as follows:[19] to a stirred solution of **1** (600 mg, 0.89 mmol, 1.0 equiv.) in DMF was added a 40 % solution of KOH (2.40 g, 0.04 mol, 50 equiv.) in water (15 mL). The reaction mixture was shielded from light and it was stirred at room temperature overnight. At reaction completion (TLC, silica gel, dichloromethane/methanol 94:6), the excess solvent was removed under reduced pressure. The resultant solid was dissolved in dichloromethane and neutralised with 5 mL of 1M HCl. The solid was redissolved in dichloromethane (50 mL) and extracted with water (2 x 50 mL). The organic fraction was evaporated under reduced pressure and the crude product was dissolved in 50 mL of dichloromethane and precipitated with 100 mL methanol affording a purple product (559 mg, 95% yield).

$\lambda_{max}(CH_2Cl_2, 25°C)$/nm 415 (ε/$dm^3mol^{-1}cm^{-1}$ 715165), 515 (52074), 550 (17556), 590 (17305) and 645 (7015).

^{1}H (400 MHz, $CDCl_3$) δ: − 3.00 (2H, s, NH), 8.00 (2H, d, *J* = 8.0 Hz, *o*Ph), 8.02-8.05 (6H, m, 3,5Py), 8.18 (2H, d, *J*= 8.0 Hz*, m*Ph), 8.65 (8H, br s, βH), 8.74-8.80 (6H, m, 2,6Py).

^{13}C (100 MHz, $CDCl_3$) δ: 178.21, 154.91, 151.61, 151.58, 147.14, 141.39, 138.13, 133.75, 131.57, 125.81, 121.11, 120.68.

ESI-MS (*m/z*) (MeOH/MeOH + diethylamine): calcd. for $C_{42}H_{26}N_7O_2$: 661.22 found $[M-H]^-$: 660.2153.

5-(4-(2-(2-(2-acrylamidoethoxy)ethoxy)ethyl)carboxyphenyl-10,15,20-tris(4-*N*-pyridyl)porphyrin (4):

To a stirred solution of **2** (100 mg, 0.15 mmol, 1.0 equiv.), 1-ethyl-3-(3-dimethylaminopropyl)carbodiimide hydrochloride (EDCI·HCl) (44.0 mg, 0.23 mmol, 1.5 equiv.) and hydroxybenzotriazole (HOBt) (31.2 mg, 0.23 mmol 1.5 equiv.) in dry DMF (5 mL) was added a solution of *N*-(2-(2-(2-aminoethoxy)ethoxy)ethyl)acrylamide (46.8 mg, 0.23 mmol, 1.5 equiv.) and 4-dimethylaminopyridine (DMAP) (31.2 mg, 0.26 mmol, 1.1 equiv.) in dry DMF (2 mL). The reaction mixture was shielded from light and stirred at room temperature under nitrogen for 24 h. At reaction completion (TLC: silica gel, dichloromethane/methanol 92:8), the solvent was removed under reduced pressure. The resulting dark solid was washed with water (3 x 50 mL) and diethyl ether (2 x 50 mL). The crude product was purified using column chromatography on silica gel using gradient elution in dichloromethane/methanol 92:8. The product **6** was obtained as a purple solid (53.0 mg, 42 % yield).

λ_{max}(CH_2Cl_2, 25°C)/nm 415 (ε/$dm^3mol^{-1}cm^{-1}$798987), 515 (50866), 545 (16064), 590 (14767) and 645 (5317).

^{1}H (400 MHz, $CDCl_3$) δ: 3.30-3.33 (2H, m, CH_2NH), 3.51 (2H, t, CH_2NHCOCH, *J* = 5.8 Hz), 3.57-3.73 (8H, m, $CH_{2\ peg}$), 5.56 (1H, dd, CH_2CHCO, J_{cis} = 10.4 Hz, J_{gem}= 1.6 Hz), 6.07(1H, dd, CH_2CHCO, J_{trans} = 17.1 Hz, J_{gem} = 1.6 Hz), 6.27 (1H, dd, CH_2C*H*CO, J_{trans} = 17.1 Hz, J_{cis} = 10.0 Hz), 8.22 (1H, t, CH_2NH, *J*= 5.0 Hz), 8.26-8.30 (6H, m, 2,6Py), 8.30-8.35 (4H, m, *o*/*m*Ph), 8.84-8.93 (8H, m, βH), 9.02-9.08 (6H, m, 3,5Py).

^{13}C (100 MHz, $CDCl_3$) δ: 166.68, 165.34, 157.08, 144.77, 143.59, 134.74, 132.68, 126.67, 125.67, 122.48, 115.96, 115.31, 70.22, 69.65, 69.58, 48.42.

ESI-MS (*m/z*) (CH_2Cl_2)/MeOH): calcd. for $C_{51}H_{43}N_9O_4$: 845.34 found $[M+ Na]^+$: 868.3330.

5-[4-(2-(2-(2-acrylamidoethoxy)ethoxy)ethyl]carboxyphenyl-10,15,20-tris(4-*N*-methylpyridyl)porphyrintrichloride (5):

To a solution of **4** (150 mg, 0.177 mmol, 1 equiv.) in DMF (50 mL) was added, *via* syringe, methyl iodide (1.50 mL, 24.1 mmol, 130 equiv.). The reaction mixture was shielded from light and stirred at 40 °C for 24 h. At reaction completion (TLC: silica gel, sat. potassium nitrate/water/acetonitrile, 1:1:8*)*, 100 mL of diethyl ether was added and the resultant precipitate was filtered off through cotton. The solid was dissolved again in 100 mL of a 10% solution of ammonium hexafluorophosphate in water. The resulting precipitate was filtered and dissolved in 100 mL of a 10% solution of tetrabutylammonium chloride in acetone. The resulting precipitate was filtered, dissolved in 10 mL of methanol and precipitated with 20 mL of diethyl ether. The workup afforded the product as a chloride salt (131 mg, 75% yield).

λ_{max}(water, 25°C)/nm 420 (ε/dm^3mol^{-1} cm^{-1}224511), 520 (13412), 560 (5726), 585 (6290) and 645 (1551).

^1H (400 MHz, DMSO-d_6) δ: -3.03 (2H, s, NH), 3.30-3.33 (2H, m, CH_2-NH), 3.52 (2H, t, CH_2-NH, *J* = 4.0 Hz), 3.57-3.74 (8H, m, CH_{2peg}), 4.72-4.75 (9H, m, N-CH_3), 5.56 (1H, dd, CH_2CHCO, J_{cis}= 10.4 Hz, J_{gem}= 2.0 Hz), 6.07 (1H, dd, CH_2CHCO, J_{trans}= 17.1 Hz, J_{gem} = 1.6 Hz), 6.29 (1H, dd, CH_2CHCO, J_{trans} = 17.1 Hz, J_{cis} = 10.0 Hz), 8.30-8.27 (1H, m, CH_2NH), 8.33 (2H, d, *o*Ph, *J*= 8.0 Hz), 8.39 (2H, d, *m*Ph, *J*=8.2 Hz), 8.98-9.06 (10H, m, 8βH + Py), 9.17 (4H, br s, Py), 9.50-9.53 (6H, m, 2,6Py).

^1H (400 MHz, D_2O) δ: 2.96 (2H, t, *J* = 5.2 Hz, $CONHCH_2$), 3.17 (2H, t, *J* = 5.2 Hz, $CH_2NHCOCH$), 3.22–3.46 (8H, m, CH_2 *peg*), 4.69 (9H, s, N-CH_3), 5.18 (1H, d, CH_2CHCO, *J* = 10.0 Hz), 5.69 (1H, d, CH_2CHCO, J_{trans}= 16.6 Hz), 5.79 (1H, dd, CH_2CHCO, J_{trans} = 17.1 Hz, J_{cis} = 10.0 Hz), 6.74 (1H, d, J = 6.1 Hz, CH_2CHCO), 6.91 (1H, d, *J* = 6.9 Hz, CH_2CHCO), 8.39 (4H, d,

J = 5.0 Hz, o/mPh), 8.60 (6H, d, J = 6.2 Hz, 3,5Py), 9.27 (8H, d, *J* = 6.0 Hz, βH), 9.27 (6H, d, *J* = 6.2 Hz, 2,6Py).

^{13}C (100 MHz, DMSO-*d*$_6$) δ: 166.68, 165.34, 157.08, 144.77, 143.59, 134.59, 134.85, 132.68, 132.31, 126.67, 122.48, 115.95, 115.31, 70.22, 69.65, 48.42.

ESI-MS (m/z) (MeOH)/MeOH): calcd. for $C_{54}H_{52}N_9O_4Cl_3$: 995.32; found $[M - 3Cl]^{3+}$: 296.8042.

HPLC: t_R : 8.40 min.

{5-[4-(2-(2-(2-acrylamidoethoxy)ethoxy)ethyl]carboxyphenyl-10,15,20-tris(4-*N*-methylpyridyl)porphyrinatotrichloride}palladium(II) (6):

To a 35 mL microwave vessel was added **5** (120 mg, 0.12 mmol, 1.0 equiv.) and palladium acetate (180 mg, 0.80 mmol, 6.7 equiv.) in a mixture of water/methanol (25 mL) (90:10). The mixture was heated at 100 °C for 2 h. At reaction completion, (TLC: silica gel, sat. potassium nitrate/water/acetonitrile, 1:1:8), the mixture was cooled and filtered through celite to remove any palladium impurities. A 10% solution of ammonium hexafluorophosphate in water was added (10 mL) and the resulting precipitate was filtered and redissolved in 100 mL of a 10% solution of tetrabutylammonium chloride in acetone. The resulting precipitate was filtered to give compound **6** as the chloride salt. The product was then dissolved in 10 mL methanol and precipitated adding 20 mL of diethylether to give **6** as a purple solid (86.5 mg, 65 % yield).

λ_{max}(water, 25°C)/nm 420 (ε/dm^{3}mol^{-1}cm^{-1} 217732), 525 (22881) and 560 (7125).

^{1}H (400 MHz,DMSO-*d*$_6$) δ: 3.30-3.33 (2H, m, CH_2-NH), 3.44-3.76 (12H, m, CH_2*peg* + CH_2-NH), 4.73 (9H, s, N-CH_3), 5.56 (1H, dd, CH_2CHCO, J_{cis} = 10.4 Hz, J_{gem}= 2.0 Hz), 6.07 (1H, dd, CH_2CHCO, J_{trans} = 17.1 Hz, J_{gem} = 1.6 Hz), 6.24-6.34 (1H, dd, CH_2CHCO, J_{trans} = 17.1 Hz, J_{cis} = 10.0 Hz), 8.37 (4H, dd, *o*/*m*Ph), 8.93-9.05 (10H, m, 8βH + 2 Py), 9.07-9.13 (4H, m, Py), 9.44-9.59 (6H, m, 2,6Py).

^{13}C (100 MHz,DMSO-*d*$_6$) δ: 156.58, 144.90, 144.69, 143.15, 142.04, 140.51, 140.18, 134.32, 132.38, 126.73, 123.78, 117.73, 70.20, 69.59, 48.45.

HPLC: t_R: 8.52 minutes

{5-[4--(2-(2-(2-acrylamidoethoxy)ethoxy)ethyl]carboxyphenyl-10,15,20-tris(4-*N*-methylpyridyl)porphyrinatotrichloride}copper(II) (7):

To a stirred solution of **5** (50.0 mg, 0.05 mmol, 1.0 equiv.) in water (8 mL) was added copper(II) sulphate pentahydrate (50.0 mg, 0.20 mmol, 4.0 equiv.). The reaction mixture was shielded from light and stirred at room temperature for 24 h. At reaction completion (TLC: silica gel, sat. potassium nitrate/water/acetonitrile, 1:1:8), 10 mL of a 10% solution of ammonium hexafluorophosphate in water was added and the resulting precipitate was filtered and redissolved in 100 mL of a 10% solution of tetrabutylammonium chloride in acetone. The resulting precipitate was filtered to give compound **7** as the chloride salt. The product was dissolved in 10 mL of methanol and precipitated with 20 mL of diethyl ether to give **7** as a purple solid (48.2 mg, 91 % yield).

λ_{max}(water, 25°C)/nm 425 (ε/$dm^3mol^{-1}cm^{-1}$ 213249), 550 (18576) and 575 (5447).

ESI-MS (m/z) (MeOH)/MeOH): calcd. for $C_{54}H_{52}N_9O_4Cl_3Cu$: 1056.24; found $[M–3Cl]^{3+}$ 317.1088.

HPLC: tR: 8.55 minutes.

Hydrogel synthesis

Synthesis of control hydrogel (8): Acrylamide (1.91 g, 26.87 mmol) and N',N'-methylene bis acrylamide (66.0 mg, 0.43 mmol) were dissolved in 6.6 mL of distilled water. To this solution was added 0.100 mL of a 10% solution of SDS (9.96 mg, 0.03 mmol) and 3.30 mL of distilled water and the mixture was gently stirred. Following this 0.100 mL of a 10% solution of APS and 0.020 mL of TEMED were subsequently added and the solution transferred into a mould (l = 3.3 cm, w = 3.3 cm, h= 1cm) and left for 15-20 mins to polymerise. The gel was then removed from the mould and then washed with distilled water and kept moist in a dust free chamber.

IR (neat): v (cm^{-1}) = 1652.2, 1606.4, 1452.6, 1325.4, 1118.0.

General method for the synthesis of porphyrin hydrogels (9, 10, 11): Acrylamide (1.91 g, 26.87 mmol) and N',N'-methylene bis acrylamide (66.0 mg, 0.43 mmol) were dissolved in 6.6 mL of distilled water. To this solution was added 0.100 mL of a 10% solution of SDS (9.96 mg, 0.03 mmol) and compound **5**, **6** or **7** (4.0 mg, 4.4 mg and 4.1 mg respectively, 3.3 mM) previously dissolved in 3.30 mL of distilled water. The mixture was gently stirred, and then 0.100 mL of a 10% solution of APS and 0.020 mL of TEMED were subsequently added and the solution transferred into a mould (l = 3.3 cm, w = 3.3 cm, h= 1cm) and left for 15-20 mins to polymerise in the dark. The gel was then removed from the mould and then washed with distilled water and kept moist in a dust-free chamber.

For hydrogel **9**:

IR (neat): v (cm^{-1}) = 1653.3, 1615.7, 1456.5, 1326.9, 1130.0.

λ_{max} (neat)/nm 425 (ε/$dm^{-3}mol^{-1}$, 52468), 520 (5957) 560 (3421) 590 (3248) and 650 (2983)

For hydrogel **10**:

IR (neat): v (cm^{-1}) = 1653.6, 1456.5.

λ_{max} (neat)/nm 420 (ε/$dm^{3}mol^{-1}$, 50359), 530 (8488) and 560 (5934).

For hydrogel **11**:

IR (neat): v (cm^{-1}) = 1636.6, 1456.4.

λ_{max} (neat)/nm 425 (ε/$dm^{-3}mol^{-1}$, 33380), 550 (5558) and 570 (3489).

Characterization of hydrogels by SEM

The morphology of the hydrogels was characterized by field emission scanning electron microscopy. Scanning electron microscope (SEM) images of the hydrogel alone **(8)** or in the presence of the porphyrin **(9, 10, 11)** were obtained using a EVO60 scanning electron microscope (Zeiss) fitted with a cryo-preparation system-model: PP3010T, manufacturer: Quorum Technologies. After plunge freezing in liquid nitrogen the sample was transferred (under vacuum) to the cryo system preparation chamber. Most of the water ice was removed by sublimation by

increasing the temperature of the sample from 140 °C to 60 °C at a pressure of 5 x10 $^{-5}$ mbar for 10 -12 minutes. After this, the temperature of the sample was reduced to -140 °C and a pressure of approximately 5 x10^{-7} mbar. The sample was then sputter coated with about 2 nm of platinum and then transferred to the SEM for examination. The SEM electron beam accelerating voltage used was 15 kV at a probe current of 20–35 pA. The diameters of the gel pores were determined using the Image J program.[20]

Antibacterial activity of hydrogels

E. coli strain DH5a contains the plasmid pGLITE, a derivative of pBBR1MCS-2 containing the lux CDABE operon of Photorhabdus luminescense was maintained from frozen stock on nutrient agar (Oxoid Ltd, Basingstoke, UK) and were grown as broth cultures using Reinforced Clostridial Medium (RCM; Oxoid Ltd Basingstoke, UK) with addition of kanamycin (10 mg L^{-1}) to selectively maintain the lux plasmids.

For experiments on photodynamic killing, microbial cells were obtained by inoculation of test species in 10 mL volumes of appropriate liquid medium and incubated in a shaking incubator (model S 150, Stuart shakers, UK) at 37° C for 4 to 6 hours to obtain mid exponential phase cultures. A total of 100 µL of bacterial suspension was appropriately diluted in 2 mL PBS (pH = 6.0) to obtain approximately 10^{6} colony-forming units (cfu) mL^{-1}.

The photoantimicrobial hydrogels (**9**, **10** or **11**) were cut into four squares and equilibrated with PBS (pH = 6.0) for 30 minutes. Then the media was discarded, the gel was washed with PBS of the same pH and placed into the diluted bacterial suspension in borosilicate glass tubes (12 by 75 mm; Fisher Scientific, Loughborough, UK) using the same tube for both light irradiation and measurement of bioluminescence light output. The samples were irradiated with a white light at a fluence rate of 14.5 mW cm^2 for 20 or 25 minutes (total light dose was either 17.4 or 21.8 J cm^2).

The illumination was performed using a fiber optic cable (F = 1 cm) and lamp (Fiber Illuminator, OSL1-EC, ThorLabsInc, Ely, Cambridgeshire) with a 150 W halogen lamp. Luminescence light

output was measured by quickly inserting the tube into a FB12 luminometer (Berthold Detection Systems, Germany) to quantify the light output as relative light units (RLU). A borosilicate tube was similarly treated, but not exposed to light and used as a reference for the dark toxicity under the same experimental conditions. The hydrogel alone (**8**) was tested following the same protocol. A control experiment on an *E. coli* suspension irradiated and in the dark indicated that light doses alone up to 21.8 J cm^{-2} cause no evident bacterial damage. All experiments were conducted in duplicate.

Results and Discussion

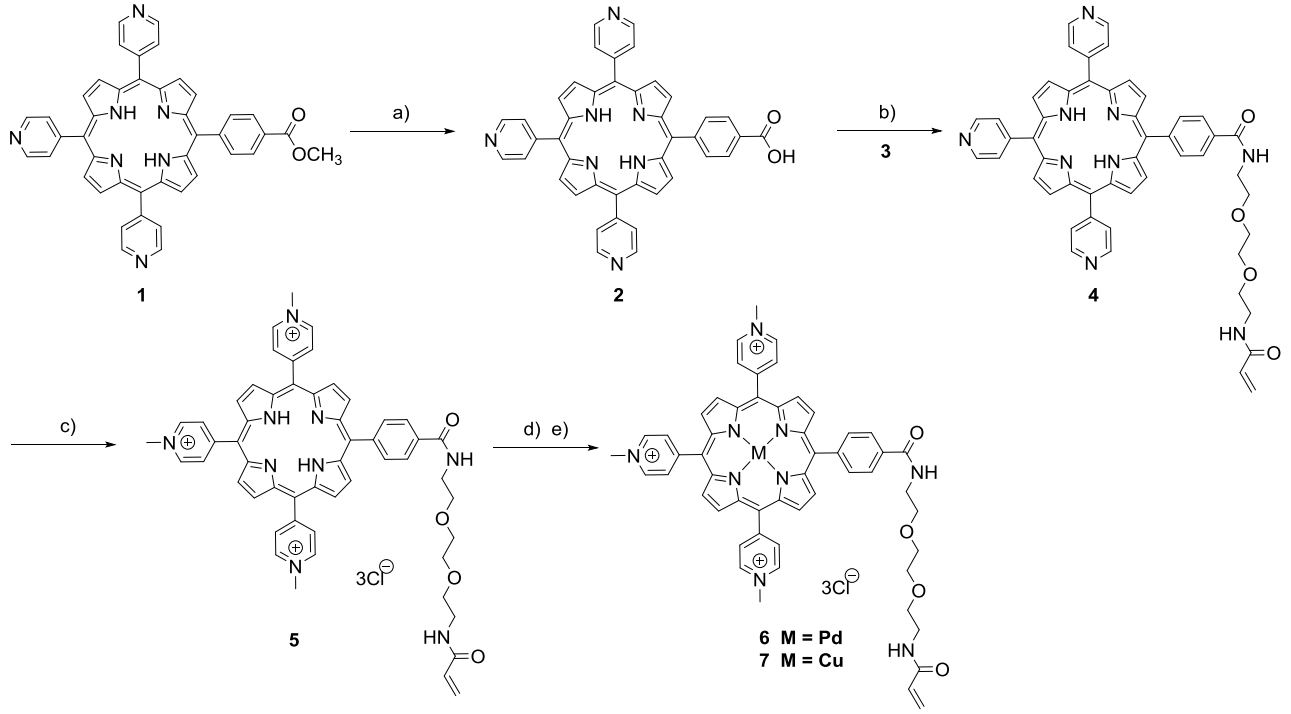

Figure 2. Synthetic Route to the water soluble 5-[4--(2-(2-(2-acrylamidoethoxy)ethoxy)ethyl]carboxyphenyl-10,15,20-tris(4-*N*-methylpyridyl)porphyrin trichloride **(5)** and to its metal derivatives {5-[4--(2-(2-(2-acrylamidoethoxy)ethoxy)ethyl]carboxyphenyl-10,15,20-tris(4-*N*-methylpyridyl)porphyrinato trichloride}palladium(II) **(6)** {5-[4--(2-(2-(2-acrylamidoethoxy)ethoxy)ethyl]carboxyphenyl-10,15,20-tris(4-*N*-methylpyridyl)porphyrinato trichloride}copper(II) **(7).**

Reactions and conditions: a) KOH, DMF/water mixture, 12h, rt, 95% yield. b) Alkyl amine, EDCI/HOBt/DMAP, dry DMF, 24 h, rt, N_2, 42% yield. c) CH_3I, DMF, 24 h, 40 °C, ammoniumhexafluorophosphate in water followed by tetrabutylammonium chloride in acetone (Cl^- counter-ion), 75 % yield. d) palladium acetate, water/methanol mixture (90:10), 100°C, 2h, microwave, 65% yield. e) copper sulphate, water, rt, 24 h, 91% yield.

The starting material, 5-(4-carboxymethylphenyl)-10,15,20-tris(4-*N*-pyridyl)porphyrin **(1)** was obtained using a relatively straightforward process, as the procedure is well established within the literature.[21] **1** was obtained by condensation of 4-pyridinecarboxyaldehyde, methyl 4-

formylbenzoate and pyrrole in a 3:1:3.5 molar ratio under Adler–Longo conditions followed by accurate chromatographic separation of the statistic mixture of the six isomeric porphyrins (having from zero to four 4'-pyridyl rings in the *meso* positions).[20,22] Hydrolysis of the ester group of **1** in DMF under basic condition gave 5-(4-carboxyphenyl)-10,15,20-tris(4-*N*-pyridyl)porphyrin (**2**) in 95% yield. The mass spectrum in negative mode of **2** provides evidence that the molecular peak is at 660.2163 (Figure S1).

Preparation of the commercially unavailable N-{2-[2-(2-aminoethoxy)ethoxy]ethyl}acrylamide (**3**), useful for the later covalent immobilization of the photosensitising unit on a polymeric support, was carried out via standard reactions as previously reported by us.[16] The mass spectrum of **3** provides evidence that the molecular peak is at 203.1387 as $(MH)^+$ (Figure S2).

The hydroxybenzotriazole (HOBt) ester of **2** was then coupled with the water soluble N-{2-[2-(2-aminoethoxy)ethoxy]ethyl}acrylamide **(3)** in DMF at rt under nitrogen overnight.

After purification by column chromatography, **4** was obtained in 42% yield and high purity and was characterized by UV–vis, ^{1}H NMR spectroscopy and by Electrospray Mass Spectrometry (Figures S3 – S5 in ESI). ^{1}H NMR and ^{13}C NMR clearly demonstrated that **4** is an asymmetric structure.

The resonances of the two equivalent pyridyl rings trans to one another are indistinguishable from those of the third pyridyl ring; similarly, the eight pyrrole protons (βH) give a single unresolved multiplet (four doublets would be expected, based on the symmetry).

In the downfield region, besides the two doublets for the pyridyl protons at δ 9.05 (2,6 Py) and 8.27 (3,5 Py) and the singlet for the *o,m* Ph protons at δ 8.31, the spectrum shows the triplet of the amide NH at δ 8.22 partially overlapping with the doublet of the 3,5 Py protons. The ^{1}H NMR spectrum of **4** shows the characteristic resonances of the acryloyl group at δ 6.26 (CH_2=C*H*CO), at δ 6.06 for the C*H*$_2$=CHCO *trans* and at δ 5.55 for the C*H*$_2$CH=CO *cis*. In the upfield region, the spectrum shows the multiplet of the alkylic chain (δ = 3.70 – 3.59) and the triplet at δ 3.51 of the C*H*$_2$NHCOCH. The two internal NH pyrrole protons appear as a relatively sharp singlet at δ ≈ - 3.0. The mass spectrum of **4** provides evidence that the molecular peak is at 868.3330 (M+ Na^+) (Fig. S5 in ESI).

Despite the presence of a flexible and hydrophilic PEG-like linker, water solubility turned out to be insufficient: good solubility was only obtained by methylation of the residual pyridyl-*N* atoms, which provided three positive charges. Methylation of **4** with excess methyl iodide in DMF gave the tricationic porphyrin **5** (as iodide salt) in almost quantitative yield. Anion exchange was carried out with ammonium hexafluorophosphate and tetrabutylammonium chloride, to give **5** as the chloride salt in 75% yield. The mass spectrum of **5** has a quite complicated pattern due to the 3^+ charge (Fig. S6 in ESI), its ^{1}H NMR spectrum confirmed its authenticity (Fig. S7 in ESI).

As mentioned above, the upfield region of the ^{1}H NMR spectrum of **5** in DMSO-d_6 is similar to that of its precursor **4**. The two internal NH pyrrole protons appear as a relatively sharp singlet at δ ≈ -3.03. Also all of the resonances of the multiplet of the alkylic chain and the resonances of the acryloyl group are not affected by the insertion of the three positive charges.

As expected, in the downfield region, the resonance of the pyridyl protons at δ 9.52 (2,6 Py) and δ 8.98 (3,5 Py) are strongly affected by the methylation showing a remarkable shift downfield by 0.5−1.0 ppm while the *o/m* Ph protons resonate as double doublet at δ 8.33. The two NH amide protons resonate at δ 9.07 and 8.29 and they are partially overlapping with the doublet of the 3,5 Py protons and with the double doublet of the *o/m*Ph, respectively.

The correlation H–H COSY spectrum of **5** (Fig. S8, ESI) displays, besides the expected cross peaks, also two long range weak correlation peaks between the aromatic protons and the CH_2 of the C1 of the alkylic chain and the NH amide proton and between the CH_2 proton of the C8 of the alkylic chain and the NH amide proton that allowed their assignment unambiguously.

Interestingly, the spectrum showed also a weak cross peak between the 2,6 Py protons and the NCH_3 that allowed their assignment unambiguously.

The downfield region of the ^{1}H-NMR spectrum of **5** in D_2O is similar to that of its ^{1}H-NMR in DMSO-d_6 except that all resonances are broader possibly due to aggregation occurring at NMR concentrations (Fig. S9, ESI). The 3,5 and 2,6 Py and β protons resonate as doublets and they are shifted upfield by 0.3 ppm. The *o/m* Ph peaks resonate as a doublet at 8.39 in D_2O while in the

DMSO-d_6 spectrum they resonate as a double doublet. The acryloyl protons δ 5.79 (CH_2=C*H*CO), δ 5.69 for the CH_2=CHCO *trans* and at δ 5.18 for the CH_2CH=CO *cis* are remarkably shifted upfield by ~ 0.4 ppm. Furthermore, the CH_2=CHCO *trans* and the CH_2CH=CO *cis* resonate as doublets while in the DMSO-d_6 they resonate as a double doublet. The NCH_3 protons partially overlap with the signal of the water. In the upfield region, the multiplet of the alkylic chain and the triplet at δ 3.17 of the CH_2NHCOCH have been shifted upfield by ~ 0.4 ppm.

Interestingly, the D_2O spectrum shows the triplet for the C1 proton at 3.17 which is not observed in the DMSO-d_6 because it overlaps with the residual peak of the DMSO.

Compound **5** gives a single HPLC peak with a retention time of 8.4 minutes (Fig. S11, ESI). The final compound **5** dissolves well in polar solvents such as methanol, water and PBS, which allows it to be used in a range of different polymeric support systems.

We decided to study the effect of insertion of a heavy atom inside the cavity of the porphyrin. Palladium was chosen to be inserted into compound **5** because Pd forms stable complexes with several porphyrins and it can be used to enhance the photodynamic action of the sensitiser[23] inducing the heavy atom effect which increases the singlet oxygen quantum yields by increasing the triplet state lifetime.

Palladium was inserted according to a modified literature method,[24] where a microwave reactor was used. Palladium acetate and the water-soluble porphyrin **5** were dissolved in a mixture of water/ methanol. The insertion of palladium was confirmed by UV-vis spectroscopy (Fig. S10 (a), ESI) where the typical four Q-bands are replaced by two Q bands at 525 and 560 nm while the Soret band remains unchanged at 420 nm (Fig. S10 (b), ESI).

Compound **6** shows a single HPLC peak at a retention time of 8.5 minutes, similar to the one obtained for the parent compound **5** (Fig. S11, ESI).

The upfield region of the ^{1}H NMR spectrum of **6** in DMSO-d_6 is similar to that of its precursor **5** except for the expected absence of the sharp singlet at δ ≈ - 3.0 of the two internal pyrrole NH. All of the resonances of the acryloyl group are not affected by the insertion of the metal inside the

cavity. In the downfield region, the resonance of the pyridyl protons at δ 9.52 (2,6 Py) and 8.98 (3,5 Py) are shifted downfield by 0.5−1.0 ppm, while the *o/m* Ph protons resonate as double doublet at δ 8.33 (Fig. S12, ESI).

We also decided to incorporate Cu(II) in the central cavity to use the Cu(II) porphyrin as a control, since most Cu(II) complexes do not display phototoxicity,[25] and so the photosensitising activity could be attributed to the Pd(II) porphyrin alone.

The insertion of copper was carried out using copper sulphate pentahydrate in water and stirring at rt for 24 h. The workup procedure was straightforward, a simple counter ion exchange to give the final compound as the chloride salt **(7)**. Copper insertion was confirmed by UV-vis (Fig. S13 (a), ESI) where the four Q-bands of the non-metallated porphyrin become two Q-bands (Fig. S13 (b), ESI).

The mass spectrum of **7** provides evidence that the molecular peak is at 317.1088 as $(M - 3Cl)^{3+}$ (Fig. S14, ESI).

Compound **7** gives a single HPLC peak with a retention time of 8.5 minutes, similar to the one obtained for the parent compound **5** (Fig. S15, ESI).

2. Synthesis and characterisation of the hydrogels

Figure 3. Photograph of 1 cm^3 of the hydrogels: (a) control hydrogel **(8),** (b) porphyrin hydrogel **(9)** with 4.0 mg of **5** (3.3 mM stock solution in PBS, pH=6.0) immobilized in it, (c) Cu(II)porphyrin hydrogel **(11)** with 4.1 mg of **7** (3.3 mM stock solution in PBS, pH=6.0) immobilized in it, (d) Pd(II) porphyrin hydrogel **(10)** with 4.4 mg of **6** (3.3 mM stock solution in PBS, pH=6.0) immobilized in it.

Polyacrylamide was chosen as the support for the incorporation of the three synthesised porphyrin photosensitisers for numerous reasons including good biocompatibility, high porosity and high permeability and optical transparency.[26,27,28,29]

The optically transparent polyacrylamide hydrogels were easily prepared by free radical polymerization of acrylamide (Am) and N,N'-methylenebisacrylamide (Bis) using ammonium persulfate (APS) and N,N,N',N'-tetramethylethylenediamine (TEMED) as the redox initiator and the catalyst respectively. Acrylamide and N,N'-methylene-bisacrylamide were used in a ratio of 19:1 (w/v %).

We previously reported the synthesis and characterization and the antibacterial activity of a polyacrylamide-based hydrogel with a new photoactive phenothiazinium compound immobilized on it.[16] The photosensitiser was incorporated covalently through the insertion of a terminal acryloyl group, suitable for the later polymerization and incorporation into a hydrogel.

Similarly, the three porphyrin photosensitisers, bearing a terminal acryloyl group, were incorporated into the hydrogel. The final molarity was kept constant for all of them (M = 3.3 mM). The photosensitiser was dissolved in 3.30 mL of water and added to the solution of monomers (6.60 mL). A surfactant (SDS) was added to the mixture to prevent any aggregation of the photosensitiser and to aid the formation of a homogenous solution. SDS has been used frequently for different photosensitisers in solution as it helps to prevent aggregation of charged compounds in solution.[30] Following the addition of the ammonium persulfate (APS) and the N,N,N',N'-tetramethyl-ethylenediamine (TEMED), the homogenous and optically transparent hydrogels were obtained after 15-20 minutes for all the porphyrins. The control gel **(8)** was obtained in a similar way, by adding the water without the photosensitiser as shown in Fig. 3. The gels were hydrated in deionised water for 24 hours, with the water being changed three times to remove any unreacted acrylic monomers.

The porphyrin polyacrylamide hydrogels showed leaching of photosensitiser when the washings were analysed. For hydrogels **9, 10, 11** the amount of leaching was found to be 0.0174 mg/ cm^3 for

9, 0.0204 mg/cm^3 for **10**, and 0.0035 mg/cm^3 for **11**. The stability of the gels was tested, and after 24 h the leaching ceased, with no additional leaching occuring. Leaching has been already observed for other porphyrin compounds when immobilized in solid supports.[31,32,33,34,35]

Carvalho *et al.* observed leaching after the formation of a porphyrin-nanomagnet hybrid material.[32] The leaching was seen when the material was washed with water, but the amount of leaching was not quantified. Alves *et al.* also observed leaching when the material was washed with solvents such as chloroform and methanol, in which the porphyrin was soluble. The leaching of the porphyrin was also not quantified in that case. The washing was carried out several times until the Soret band was no longer present in the absorption spectrum.[31] Leaching of the porphyrin from the support have been observed, but the amount was not quantified.[30,31,32,33,34] Gonzalez-delgado *et al.*[36] measured the leaching of their porphyrin photosensitiser by measuring the decrease in absorption of the Soret band over time and they found that over six months there was a 14% decrease in the Soret band.

The pH of the system was also investigated to see if it had an effect on the leaching of the photosensitiser. The leaching was found to be lower at a lower pH, and pH = 6.0 was therefore selected for bacterial testing.

The solid absorption spectra were obtained by the formation of the hydrogel inside the cuvette. The hydrogel was synthesised using the same method described above apart from on a smaller scale to fit the 3 mL cuvette. In general the absorption spectra for the porphyrins as solid gave broader peaks compared to the spectrum seen in solution.

The absorption spectrum of **9** as a solid shows a characteristic porphyrin spectrum with the Soret band at 425 nm, which has been red shifted by 5 nm compared to **5** in PBS solution (pH = 6.0) (Fig. S16). The absorption spectrum also shows the typical four Q-bands, the final two have been red shifted from 560 nm to 565 nm and from 645 to 650 nm respectively.

The absorption spectrum of **10** as a solid shows a characteristic porphyrin spectrum with the Soret band at 420 nm, which is the same when compared to **6** in PBS solution (pH = 6.0) (Fig. S17, ESI). The absorption spectrum also shows the typical two Q-bands expected for a palladium porphyrin,

the first Q-band is red shifted by 5 nm from 525 nm to 530 nm and the second Q-band remains the same as **7** in PBS (pH = 6.0) at 560 nm. The UV-vis spectrum is similar to **6** in PBS (pH = 6.0) which shows peaks at 420 nm, 525 nm and 560 nm, but the absorption spectrum of the solid also shows the formation of a third Q-band at 610 nm, which is not seen for the palladium porphyrin in solution. We speculate that this is due to a change in symmetry of the porphyrin. Palladium usually sits co-planar in the porphyrin,[33,37,38] but when in solid the symmetry may change due to distortion of the porphyrin molecule which could be due to the polymerization step or the different subtituents in the *meso* positions.

The absorption spectrum of **11** as a solid shows the Soret band at 425 nm, which is the same when compared to **7** in PBS solution (pH = 6.0) (Fig. S18, ESI) and the typical two Q-bands expected for a Cu(II)porphyrin, the first Q-band remains at 550 nm but the second Q- band has been blue shifted from 575 nm to 570 nm. The UV-vis spectrum is similar to **7** in PBS (pH = 6.0) which shows peaks at 425 nm, 550 nm and 575 nm.

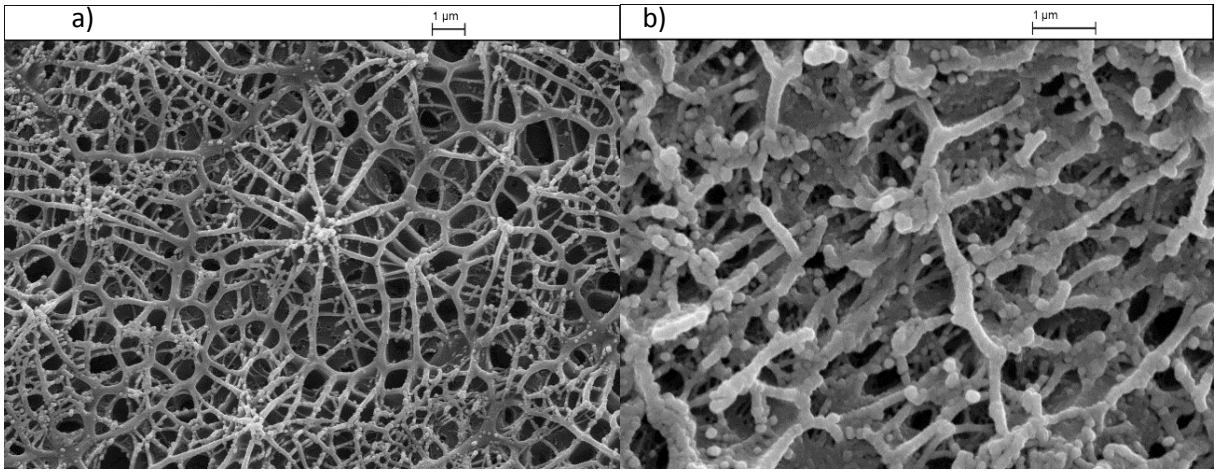

Figure 4a. Scanning electron microscope (SEM) image of control hydrogel **8**.

Figure 4b. Scanning electron microscope (SEM) image of photoantimicrobial hydrogel **9**.

The morphologies of all the hydogels was investigated by scanning electron microscopy (SEM).

For the blank hydrogel containing no photosensitiser a continous and non-ordered microporous mesh like network was observed with a mean diameter of 123 ± 14 nm (Figure 4a). Similarly, the SEM of **9** showed a continous and porous mesh like structure, but with less order. Within this less ordered structure there is a finer mesh like non-ordered porous structure. The mean pore diamater was found to be 140 ± 30 nm (Figure 4b).

3. Antibacterial activity

The testing of the hydrogels against bacteria carried out in this work was aimed at understanding the bacterial killing properties of three different porphyrins immobilized on the same support.

For a preliminary evaluation of the photo-induced antibacterial activity of the previously synthesized hydrogels, the Gram-negative *E. coli*, was chosen as a representative Gram-negative bacterium, some strains of which can be important human and animal pathogens.[39]

The use of lux-bioluminescent target cells, coupled with luminometry provides many advantages over conventional methods of assessing kill rates which involve viable count methods that are slow to perform and less accurate. Using bioluminescence avoids the need for sub-samples, serial dilutions, plating, incubation and counting of recovered colonies.

PACT for the immobilized porphyrin hydrogels was evaluated in PBS (pH =6.0).

In a preliminary experiment, three hydrogels with an increasing concentration of **5** were tested to find the optimum concentration of porphyrin immobilized on the polyacrylamide gel. (Fig. S19, ESI). 1 cm square with 1 mg/cm^3 of porphyrin immobilized, 2 mg/cm^3 gel and 4 mg/cm^3 of porphyrin immobilized were cut into four equal pieces and they were placed in 2 mL of PBS (pH = 6.0) for 30 minutes to equilibrate. After this the solution was discarded and the hydrogel was added to the broth of *E. coli* in PBS (2000 μl). The measurements were taken every minute for both the sample under irradiation with white light and the sample in the dark.

The 4.0 mg/cm^3 gel (M = 3.3 mM) was found to be the most active with a log reduction in the light of 1.590 after 20 minutes, whereas the 2.0 mg/cm^3 and the 1.0 mg/cm^3 hydrogels showed reductions of 1.158 and 0.908 after 20 minutes respectively.

Therefore, the 4.0 mg/cm^3 gel (M = 3.3 mM) **(9)** was selected for the further experiments. The other hydrogels **10** and **11** were therefore tested keeping the same molarity.

The photo-induced antibacterial activity of hydrogels **9** and **10** and **11** was then assessed against the model organism, the Gram-negative *E. coli*.

Thus, the three hydrogels **9**, **10** and **11** cut in four pieces were placed inside of the cell suspension in culture tube containing ~2 × 10^6 CFU ml^{-1}CFU/mL and irradiated with visible light for different times.

The results (Figure 5) clearly indicate that the microorganisms are rapidly photoinactivated when the cultures in the presence of the photoantimicrobial hydrogels are exposed to visible light.

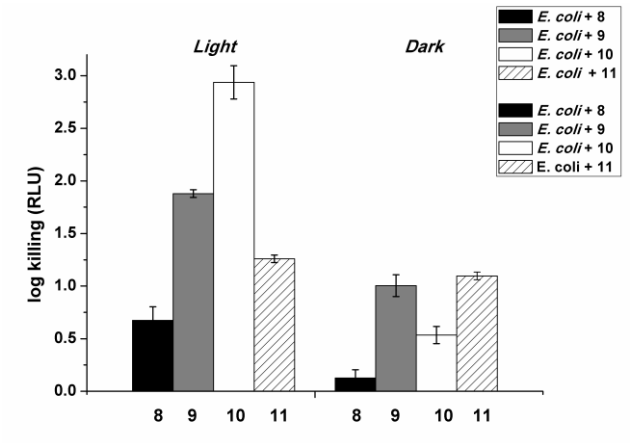

Figure 5. Biocidal activity of the photoantimicrobial porphyrin hydrogel **(9)**, Pd(II)porphyrin hydrogel **(10)** and Cu(II)porphyrin hydrogel **(11)** previously cut in four squares towards *E. coli* in the dark and under light illumination for 25 mins (fluence rate of 14.5 mW cm^{-2} and a total light dose 21.8 J cm^{-2}). The hydrogel without the PS **(8)** was used as control in the same experimental conditions. Dark and light experiments were done with the cell suspensions of 2 × 10^6 CFU ml^{-1}. The optical fiber was placed 6 cm from the plates. Values represent the mean of two separate experiments. Black bars correspond to the experiments done adding the control hydrogel **(8)** to the *E. coli* suspensions. Grey bars correspond to the experiments done adding the photoantimicrobial hydrogel **(9)** to the *E. coli* suspension. White bars correspond to the experiments done adding the

Pd(II)porphyrin hydrogel **(10)** to the *E. coli* suspensions while white bars with left oblique lines correspond to the experiments done adding the Cu(II)porphyrin hydrogel **(11)** to the *E. coli* suspensions. On the right are reported the experiments done in the same way without the illumination.

All of the porphyrin hydrogels exhibit a photosensitizing activity causing a decrease of *E. coli* survival after 25 mins of irradiation.

The Gram-negative bacterium *E. coli* exhibited a decrease of 1.87 log after 25 mins irradiation for **9** with a kill rate of 0.069 and 1 log reduction after 14 minutes.

The Pd(II)porphyrin hydrogel **(10)** caused a 2.93 log decrease in the survival of the *E. coli* after 25 minutes irradiation (kill rate = 0.106 and 1 log reduction after 11 minutes) using the same experimental conditions while 1.26 log decrease was observed after 25 minutes when the Cu(II)porphyrin hydrogel **11** was used (kill rate of 0.047 and 1 log decrease after 20 minutes).

Dark toxicity was found to be low in all cases and similar for the hydrogels **9** and **11** (kill rate of 0.040 and 0.047 with 1.00 and 1.09 log decrease after 25 minutes respectively), and lower for **10** (0.020 kill rate and 0.53 log decrease after 25 minutes).

The control **(8)** was able to cause a reduction in the *E. coli* (0.67 log reduction after 25 minutes, kill rate of 0.029) when exposed to the same light irradiation, while in the dark almost no bacterial killing was observed (0.12 log reduction after 25 minutes, kill rate of 0.004). Those results are in agreement with those previously obtained by us, where the hydrogel, prepared in the same way, was tested in similar conditions.[16] Since from the singlet oxygen test already performed by us on **8**, the control **(8)** was found not to be able to produce singlet oxygen when irradiated, the mechanism involved in the killing is unknown.

Control experiments on *E. coli* in PBS at pH=6.0 showed that the viability of *E. coli* was unaffected by illumination alone or by dark incubation with the hydrogels in PBS at pH=6.0 (Figure S20, ESI).

The biological results showed that Pd(II)porphyrin hydrogel **10** was the most effective material against *E. coli* while hydrogels **9** and **11** showed a similar behavior.

This behavior is in agreement with the intrinsic electronic properties of the metal – porphyrin complexes. In fact, Pd(II) is known to enhance the photodynamic action of the sensitiser, inducing the heavy atom effect which increases the singlet oxygen quantum yields by increasing the triplet state lifetime, allowing energy transfer to molecular oxygen and increasing the generation of ROS. The triplet state lifetime of Cu(II) porphyrin instead is short and quickly decays back to the ground state, preventing the generation of reactive oxygen species (ROS) by energy transfer.

Cu(II) porphyrin hydrogel **11** can be therefore used as an indicator to study the bacterial damage caused by the production of ROS. Therefore the photosensitising activity of the hydrogels **9** and **10** can be attributed to ROS, while the killing ability of **11** may involve different interaction with the external bacterial cell wall since most Cu(II) complexes do not display phototoxicity.[25]

When the three porphyrins **5**, **6**, **7** in an unbound state were used under the identical experimental condition, a similar behavior was observed (Figure 6).

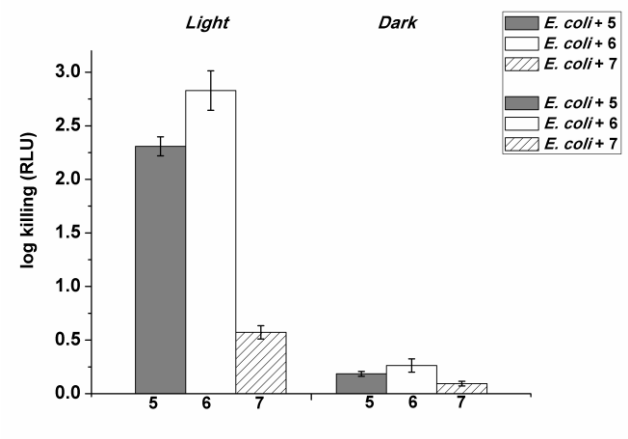

Figure 6. Biocidal activity of **5**, **6**, **7** in solution towards *E. coli* in the dark and under light illumination for 25 mins (fluence rate of 14.5 mW/cm^{-2} and a total light dose 21.8 J/cm^2). Dark and light experiments were done with the cell suspensions of 2 × 10^6 CFU ml^{-1}. The optical fiber was placed 6 cm from the plates. Values represent the mean of two separate experiments. Grey bars

correspond to the experiments done adding the cationic water-soluble porphyrin **5** to the *E. coli* suspension. White bars correspond to the experiments done adding the cationic water soluble Pd(II)porphyrin **(6)** to the *E. coli* suspensions while white bars with left oblique lines corresponds to the experiments done adding the tricationic water soluble Cu(II)porphyrin **(7)** to the *E. coli* suspensions. On the right are reported the experiments done in the same way without the illumination.

The Pd(II)porphyrin **6** caused a 2.82 log drop in survival of *E. coli* after 25 minutes of irradiation (kill rate of 0.093 and 1 log reduction after 9 minutes) while a 2.30 log drop and 0.57 log drop in survival of *E. coli* after 25 minutes of irradiation were observed when porphyrin **5** and its copper derivative **6** were tested (kill rate of 0.120 and 0.019 respectively and 1 log reduction for **5** after 11 minutes).

Also in this case the Cu(II)porphyrin **(7)** was found to be the least active, since most Cu(II) complexes do not display phototoxicity.[25]

In the dark no bacterial killing was observed for **5** and **6**, while only a negligible decrease was observed for **7** (0.09 log reduction after 20 minutes).

The efficient and fast photoinactivation of *E. coli* in suspension prompted us to investigate the effects of recovering the hydrogels following the photoexcitation of **9** and **10** hydrogels for 20 minutes, and repeating the assays with fresh target cells each time, over a total of five cycles (Figure 7).

a) Light **(9)**

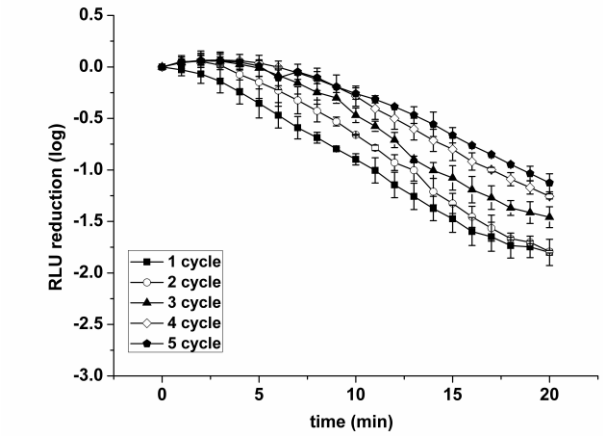

a) Light **(10)**

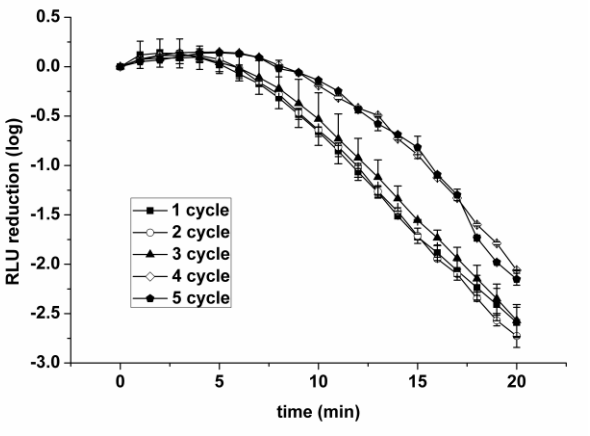

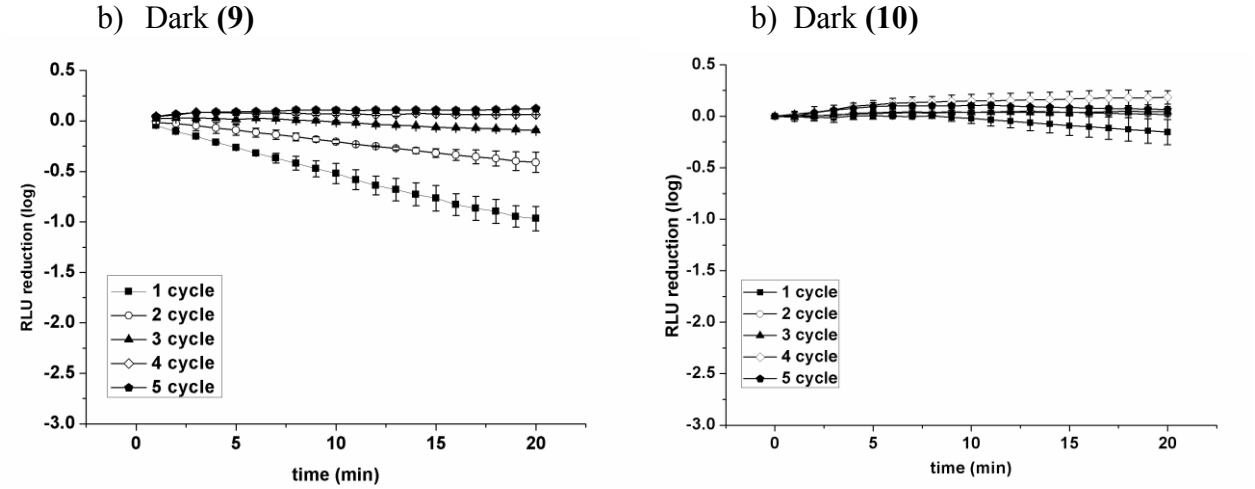

Figure 7. Kill curves obtained for the photoantimicrobial hydrogel **(9)** and **(10)** against *E. coli* over a total of five cycles both under light illumination (a) for 20 mins (fluence rate of 14.5 mW/cm^{-2} and a total light dose 17.4 J/cm^2) and in the dark (b). Dark and light experiments were done with the cell suspensions of 2 × 10^6 CFU ml^{-1}. The optical fiber was placed 6 cm from the plates. Values represent the mean of two separate experiments. The filled squares correspond to the killing curve obtained for cycle n. 1, the open circles correspond to the killing curve obtained for cycle n. 2, the filled triangles correspond to the killing curve obtained for cycle n. 3, the open rhombus correspond to the killing curve obtained for cycle n. 4, the filled pentagon corresponds to the killing curve obtained for cycle n. 5.

As before photoantimicrobial hydrogels **(9)** and **(10)** were cut in four squares and equilibrated for 30 mins in the PBS buffer at pH=6.0. Then the media was discarded, each gel was washed with PBS of the same pH and it was added to a suspension of *E. coli* cells diluted with PBS at pH = 6.0 (2 × 10^6 CFU ml^{-1}).

The bacterial light output was recorded every minute under irradiation with white light for 20 mins and in the dark. After each cycle the media was discarded, the gel was extensively washed with PBS and reused adding the same squares into a fresh *E. coli* suspension diluted with PBS (pH = 6.0).

After the first cycle, the photoactivated gel **(9)** reduced the number of surviving bacterial cells to 2 × 10^4 CFU ml^{-1} (1.80 log decrease after 20 minutes, killing rate of 0.086 and 1 log reduction after 11 minutes) (Figure 6a).

After the first cycle, the photoactivated gel **(10)** reduced the number of surviving bacterial cells to 2 × 10^3 CFU ml^{-1} (2.85 log decrease after 20 minutes, killing rate of 0.097 and 1 log reduction after 11 minutes) (Figure 6a).

The gels were then extensively washed with PBS and the photoactivated hydrogels were re-used for the disinfection of a newly prepared bacterial suspension containing the same amount of cells (2 × 10^6 ml^{-1}).

Following a 20 mins irradiation time, the same reduction of ca 1.80 log (to 3 × 10^4CFU ml^{-1}) in the viability of the bacterial cells was again achieved (killing rate of 0.086) for hydrogel **9**. Also hydrogel **10** maintained its killing ability (2.73 log decrease after 20 minutes, killing rate of 0.099 and 1 log reduction after 12 minutes).

After the third cycle, an appreciable reduction of ca. 1.45 log in the viability of the bacterial cells was again observed after 20 minutes (killing rate of 0.060) for **9** while hydrogel **10** still kept the same killing ability observed during the first cycle (2.56 log decrease after 20 minutes, killing rate of 0.090 and 1 log reduction after 13 minutes).

After the fourth and fifth cycles, a reduction of ca. 1.25 log and 1.12 log in the viability of the bacterial cells was again observed after 20 minutes (killing rate of 0.046 and 0.039 respectively) for **9** while after the fourth and fifth cycles cycle, the photoactivated gel **(10)** was still able to reduce the number of surviving bacterial cells to 1 × 10^4 CFU ml^{-1} in both cases (2.06 and 2.15 log decrease after 20 minutes, killing rate of 0.058 and 0.059 respectively and 1 log reduction after 16 minutes).

In the dark, the hydrogel **9** showed a similar killing behavior, showing a reduction of 0.96 log after 20 minutes (to 1.8 × 10^5CFU ml^{-1}, killing rate of 0.047) after the first cycle, and still showing an appreciable reduction of 0.41 log (killing rate of 0.019) after the second cycle. After the third cycle

a modest reduction of ca. 0.09 log in the viability of the bacterial cells was again observed (killing rate of 0.002) whilst the gel showed no activity during the fourth and fifth cycle (Figure 7b).

As already observed in the first experiment, hydrogel **10** showed a lower dark toxicity, when compared to the hydrogel **9** with immobilized the parent compound **(5)**. In the dark, the hydrogel **10** showed only a modest reduction of 0.15 log after 20 minutes (to 1×10^5CFU ml^{-1}, killing rate of 0.005) after the first cycle, whilst the gel showed no activity during the second, third fourth and fifth cycles (Figure 7b).

No porphyrin dyes was observed to be released from the gel as a consequence of the five irradiation sessions.

Conclusions

In the present study, we reported the synthesis, purification and characterisation of a novel cationic versatile porphyrin, namely 5-[4--(2-(2-(2-acrylamidoethoxy)ethoxy)ethyl]carboxyphenyl-10,15,20-tris(4-N-methylpyridyl)porphyrintrichloride **(5)** and of its copper and palladium derivatives, and {5-[4--(2-(2-(2-acrylamidoethoxy)ethoxy)ethyl]carboxyphenyl-10,15,20-tris(4-N methylpyridyl)porphyrinatotrichloride}palladium(II) **(6)** and {5-[4--(2-(2-(2-acrylamidoethoxy)ethoxy)ethyl]carboxyphenyl-10,15,20-tris(4-N-methylpyridyl)porphyrinatotrichloride}copper(II) **(7)** with a multistep approach and reasonable overall yield.

Those cationic porphyrins, that bear at the meso positions three quaternarised pyridyl rings and one terminal acryloyl group connected through a flexible hydrophilic linker, were particularly suited for the later polymerization and incorporation into a hydrogel.

Subsequently, three photosensitive polyacrylamide hydrogels were successfully prepared by covalently binding three cationic porphyrins into a polyacrylamide hydrogel according to a previously published strategy.

Three optically transparent polyacrylamide hydrogels were prepared by free radical polymerization of acrylamide (Am) and N,N'-methylenebisacrylamide using ammonium persulfate (APS) and N,N,N',N'-tetramethylethylenediamine (TEMED) as the redox initiator and the catalyst respectively. The hydrogel matrix resulted for all of them in a homogeneous and stable conjugate with a leaching of 0.0174 mg/ cm^3 for **9** (nmP), 0.0204 mg/cm^3 for **10** (PdP), and 0.0035 mg/cm^3 for **11** (CuP) after 30 minutes equilibration. No porphyrin dyes was observed to be released from the gel after the first washing.

The hydrogel were characterized by IR and scanning electron microscopy (SEM) and incorporation of the dye confirmed by UV - visible spectroscopy.

SEM pictures confirmed that all the hydrogels with, and without, the PS are porous structures, allowing a large surface area and thus increasing contact between the gel and the bacteria.

Promising results were obtained in our investigation of the ability of **9**, **10**, and **11** to photoinactivate bacteria. All the photoactive hydrogels successfully killed *E. coli* and the use of bioluminescent target species allowed many variables to be tested such as the effects of testing the porphyrins in solution as well as the recovery and further testing of gel through five cycles of fresh challenge.

Of the three hydrogels studied, the conjugate **10** of polyacrylamide and the palladium(II)porphyrin **(6)** proved to be the best with a 2.93 log decrease in the survival of the *E. coli* after 25 minutes irradiation. **10** showed also the lowest dark toxicity among all the three hydrogels when tested in the same conditions and the hydrogel was found to be active for five cycles, suggesting the possibility of reuse.

Further tests using more bacterial strains, viruses and fungi will be required to understand the applicability of the hydrogel in real conditions, where the water can be infected by many different species of microorganism.

The synthesized gels meet the intention to use these materials as inexpensive practical systems for water disinfection suitable in remote regions of the world, to provide small but constant amounts of sterile water. Stability studies are also planned to verify the shelf life of these materials under ambient conditions, which will be important if they are to be used in remote regions of the developing world where healthcare facilities are minimal.

Acknowledgements

The authors would like to thank EPSRC Mass Spectrometry Service, Swansea for analyses.

C.S. thanks Dr. Saliha Saad and Mr Keith Hewett for their help with the bacterial strain cultures and Mr. Tony Sinclair for the helpful discussion for the SEM interpretation.

Supplementary data

Supplementary data, including Figures S1 to S20 are available as Electronic supplementary information (ESI).

References

1 R. Laxminarayan, A. Duse, C. Wattal, A.K.M. Zaidi, H. F. L. Wertheim, N. Sumpradit, E. Vlieghe, G. L. Hara, I. M. Gould, H. Goossens, C. Greko, A. D. So, M. Bigdeli, G. Tomson, W. Woodhouse, E. Ombaka, A. Q. Peralta, F. N. Qamar, F. Mir, S. Kariuki, Z. A. Bhutta, A. Coates, R. Bergstrom, G. D. Wright, E. D. Brown and O. Cars, *Lancet. Infect. Dis.,* 2013, **13**, 1057-1098.

2 M. Wainwright, *J. Antimicrob. Chemother.,* 1998, **42**, 13-28.

3 M. R. Hamblin and T. Hasan, *Photochem. Photobiol. Sci*., 2004, **3**, 436-450.

4 P. W. Taylor, P. D. Stapleton and J. P. Luzio, *Drug Discovery Today*, 2002, **7**, 1086–1091.

5 T. Dai, Y. Y. Huang and M. R. Hamblin, *Photodiagn. Photodyn. Ther.,* 2009, **6**, 170-188.

6 M. Wainwright and K. B. Crossley, *Int. Biodeterior.Biodegrad.,* 2004, **53**, 119-126.

7 M. Wainwright, *Photodiagn. Photodyn. Ther*., 2009, **6**, 167-169.

8 A. Tavares, C. M. B. Carvalho, M. A. Faustino, M. G. P. M. S. Neves, J. P. C. Tomé, A. C. Tomé, J. A. S. Cavaleiro, A. Cunha, N. C. M. Gomes, E. Alves and A. Almeida, *Mar. Drugs*, 2010, **8**, 91-105.

9 E. Caruso, S. Banfi, P. Barbieri, B. Leva and V. T. Orlandi, *J. Photochem. Photobiol., B*, 2012, **114**, 44-51.

10 G. Jori, *J. Environ. Pathol. Toxicol. Oncol*., 2006, **25**, 505-519.

11 C. Spagnul, L.C. Turner and R. W. Boyle, *J. Photochem. Photobiol., B*, 2015, **150**, 11-30.

12 M. C. DeRosa and R. J. Crutchley, *Coord. Chem. Rev.*, 2002, **233-234**: 351-371.

13 E. Alves, M. A. F. Faustino, M. G. P. M. S. Neves, A. Cunha, H. Nadais and A. Almeida, *J. Photochem. Photobiol., C,* 2015, **22**, 34-57.

14 G. Jori, M. Camerin, M. Soncin, L. Guidolin and O. Coppellotti in *Photodynamic Inactivation of Microbial Pathogens. Medical and Environmental Applications*, ed. M. R Hamblin and ed. G Jori, The Royal Society of Chemistry, Cambridge, I edition, 2011, 1: 1-18.

15 F. Javed, L. P Samaranayake and G. E Romanos, *Photochem. Photobiol. Sci.*, 2014, **13**, 726–734.

16 C. Spagnul, J. Greenman, M. Wainwright, Z. Kamil and R.W. Boyle, *J. Mater. Chem. B*, 2016, **4**, 1499-1509.

17 R. M. Thorn, S .M. Nelson and J. Greenman, *Antimicrob. Agents Chemother.*, 2007, **51**, 3217-3224.

18 D. B. G. Williams and M. Lawton, *J. Org. Chem.*, 2010, **75**, 8351–8354.

19 Y. Ishikawa, A. Yamashita and T. Uno, *Chem. Pharm. Bull. (Tokyo)*, 2001, **49**, 287–293.

20 R. Aston, K. Sewell, T. Klein, G. Lawrie, L. Grondahl, *Eur. Polym. J*., 2016, **82**, 1-15.

21 A. D. Adler, F. R. Longo, J. D. Finarelli, J. Goldmacher, J. Assour, L. Korsakoff, *J. Org. Chem.,* 1967, **32**, 476-476.

22 T. Gianferrara, D. Giust, I. Bratsos, E. Alessio, *Tetrahedron,* 2007*,* **63**, 5006–5013.

23 D. Lazzeri, M. Rovera, L. Pascual, N. E. Durantini, *Photochem. Photobiol.,* 2004 ,**80**, 286–293.

24 F. Giuntini, V. M. Chauhan, J. W. Aylott, G. A. Rosser, A. Athanasiadis, A. Beeby, A. J. MacRobert, R. A. Brown, R. W. Boyle, *Photochem. Photobiol. Sci*., 2014, **13**, 1039-1051.

25 P. M. Antoni, A. Naik, I. Albert, R. Rubbiani, S. Gupta, P. Ruiz-Sanchez, P. Munikorn, J. M. Mateos, V. Luginbuehl, P. Thamyongkit, U. Ziegler G. Gasser, G. Jeschke and B. Springler, *Chem. Eur. J.,* 2015, **21**, 1179-1183.

26 N. A. Peppas, J. Z. Hilt, A. Khademhosseini and R. Langer, *Adv. Mater.*, 2006, **18**, 1345–1360.

27 J. Kopeček, *Biomaterials*, 2007, **28**, 5185–5192.

28 M. Hamidi, A. Azadi, P. Rafiei, *Adv. Drug Delivery Rev.*, 2008, **60**, 1638-1649.

29 A. S. Hoffman, *Adv. Drug Delivery Rev.*, 2012, **64**, 18–23.

30 B. Wilson, M. Fernandez, A. Lorente, K. B. Grant, *Org. Biomol. Chem.,* 2008, **6**, 4026-4035.

31 E. Alves, J. M. M. Rodrigues, M. A. F. Faustino, M. G. P. M. S. Neves, J. A. S. Cavaleiro, Z. Lin, Â. Cunha, M. H. Nadais, J. P. C. Tomé and A. Almeida, *Dyes Pigm.*, 2014, **110**, 80–88.

32 C. M. B. Carvalho, E. Alves, L. Costa, J. P. C. Tomé, M. A. F. Faustino, M. G. P. M. S. Neves, A. C. Tomé, J. A. S. Cavaleiro, A. Almeida, A. Cunha, Z. Lin and J. Rocha, *ACS Nano*, 2010, **4**, 7133–7140.

33 M. Magaraggia, G. Jori, M. Soncin, C. L. Schofield and D. A. Russell, *Photochem. Photobiol. Sci.*, 2013, **12**, 2170-2176.

34 C. Ringot, V. Sol, M. Barrière, N. Saad, P. Bressollier, R. Granet, P. Couleaud, C. Frochot and P. Krausz, *Biomacromolecules*, 2011, **12**, 1716–1723.

35 E. Feese, H. Sadeghifar, H. S. Gracz, D. S. Argyropoulos and R. A. Ghiladi, *Biomacromolecules*, 2011, **12**, 3528–3539.

36 J. A. González-Delgado, P. M. Castro, A. Machado, F. Araújo, F. Rodrigues, B. Korsak, M. Ferreira, J. P. C. Tomé and B. Sarmento, *Int. J. Pharm.*, 2016, **510**, 221–231.

37 M. L. Dean, J. R. Schmink, N. E. Leadbeater and C. Brückner, *Dalton Trans.*, 2008, 1341-1345.

38 M. O. Senge and M. Zawadzka, *Acta Crystallogr., Sect. C: Struct. Chem.*, 2014, **70**, 1143–1146.

39 J. B. Kaper, J.P. Nataro, H. L. Mobley, *Nat. Rev. Microbiol.,* 2004, **2**, 123-140.